Band Dependent Interlayer f-Electron Hybridization in CeRhIn$_5$

Q. Y. Chen,[1,2] D. F. Xu,[1] X. H. Niu,[1] R. Peng,[1] H. C. Xu,[1] C. H. P. Wen,[1] X. Liu,[1] L. Shu,[1] S. Y. Tan,[2] X. C. Lai,[2] Y. J. Zhang,[3,4] H. Lee,[3] V. N. Strocov,[5] F. Bisti,[5] P. Dudin,[6] J.-X. Zhu,[7] H. Q. Yuan,[3,4,8] S. Kirchner,[3,*] and D. L. Feng[1,8,†]

[1]*State Key Laboratory of Surface Physics and Department of Physics, Fudan University, Shanghai 200433, China*
[2]*Science and Technology on Surface Physics and Chemistry Laboratory, Mianyang 621908, China*
[3]*Center for Correlated Matter, Zhejiang University, Hangzhou 310058, China*
[4]*Department of Physics, Zhejiang University, Hangzhou 310027, China*
[5]*Swiss Light Source, Paul Scherrer Institute, CH-5232 Villigen, Switzerland*
[6]*Diamond Light Source, Harwell Science and Innovation Campus, Didcot OX11 0DE, United Kingdom*
[7]*Theoretical Division and Center for Integrated Nanotechnologies, Los Alamos National Laboratory, Los Alamos, New Mexico 87545, USA*
[8]*Collaborative Innovation Center of Advanced Microstructures, Nanjing 210093, China*

A key issue in heavy fermion research is how subtle changes in the hybridization between the $4f$ ($5f$) and conduction electrons can result in fundamentally different ground states. CeRhIn$_5$ stands out as a particularly notable example: when replacing Rh with either Co or Ir, antiferromagnetism gives way to superconductivity. In this photoemission study of CeRhIn$_5$, we demonstrate that the use of resonant angle-resolved photoemission spectroscopy with polarized light allows us to extract detailed information on the $4f$ crystal field states and details on the $4f$ and conduction electron hybridization, which together determine the ground state. We directly observe weakly dispersive Kondo resonances of f electrons and identify two of the three Ce $4f^1_{5/2}$ crystal-electric-field levels and band-dependent hybridization, which signals that the hybridization occurs primarily between the Ce $4f$ states in the CeIn$_3$ layer and two more three-dimensional bands composed of the Rh $4d$ and In $5p$ orbitals in the RhIn$_2$ layer. Our results allow us to connect the properties observed at elevated temperatures with the unusual low-temperature properties of this enigmatic heavy fermion compound.

It is well known that the coupling of f electrons in intermetallic rare earth (and actinide) compounds to conduction electrons can give rise to Kondo scattering processes, which commonly results in narrow bands near the Fermi energy (E_F). The correspondingly large effective mass and heat capacity over temperature (T) ratio at low T give this materials class its name: heavy fermions [1]. The great variety of possible ground states occurring in these materials has made them an ideal test bed for exploring strong correlations. As a result, a global phase diagram of heavy fermion systems has started to emerge [2,3] that is considerably richer than originally anticipated [4].

The CeMIn$_5$ heavy electron family, whose members are formed out of alternating MIn$_2$ (M = Co, Rh, Ir) and CeIn$_3$ layers, typifies this richness [5,6]. Both CeCoIn$_5$ and CeIrIn$_5$ are superconductors, with T_c's of 2.3 K and 0.4 K, respectively [7,8], while CeRhIn$_5$ is an antiferromagnet with predominantly localized moments and a Néel temperature $T_N = 3.8$ K at ambient pressure [9]. Rh lies between Co and Ir in the Group VIII elements, suggesting that already minute changes can yield drastically different ground states. This does raise the question of what determines the location of a compound in the global phase diagram, and thus the ground state. For CeCoIn$_5$, the quasiparticle bands have been directly observed by angle-resolved photoemission spectroscopy (ARPES), which indicates that the $4f$ electrons are delocalized and participate in the electronic properties at sufficiently low T [10–13]. Dynamical mean-field theory (DMFT) calculations for the quasiparticle spectral weight suggest that while the Ce $4f$ electrons in CeRhIn$_5$ are more localized than in CeCoIn$_5$, they still undergo Kondo screening with a subsequent Fermi volume enlargement at low T [14], suggesting that the ground states of both compounds possess a large Fermi surface (FS) which includes the Ce $4f$ electrons. In contrast, de Haas–van Alphen (dHvA) oscillations for CeRhIn$_5$ are essentially the same as those for LaRhIn$_5$, indicating that the Ce $4f$ electrons are localized [15,16], which is supported by optical conductivity data [17]. This is interpreted as an absence of Kondo screening in CeRhIn$_5$ at ambient pressure and is consistent with the occurrence of unconventional quantum criticality featuring critical Kondo destruction [18–20]. This interpretation has, however, been challenged in Ref. [21]. In addition, nonresonant ARPES investigations of CeRhIn$_5$ find that $4f$ electrons are predominantly itinerant [22],

while another ARPES study suggests that they are *nearly* localized in the paramagnetic state [23], and a recent scanning tunneling spectroscopy (STS) study reported the absence of a hybridization gap for CeRhIn$_5$ [24]. How can one reconcile these findings? Differences between members of the 115 family can arise from variations in the conduction (or c) electron band structure and the strength of the $4f$-multiplet c-electron hybridization. This determines the crystal electric field (CEF) splittings and the Kondo scale T_K, which affect the low-energy properties of dense Kondo systems [13].

Here we focus on the temperature range between 180 and 8 K above the Néel temperature. Combining bulk-sensitive soft x-ray ARPES, resonant ARPES, and density functional theory (DFT) calculations, we (i) unravel the three-dimensional (3D) electronic structure of CeRhIn$_5$, (ii) show that spin flip scattering in CeRhIn$_5$ results in the buildup of Kondo resonances, (iii) demonstrate that resonant ARPES with polarized light allows for the extraction of orbital information of CEF levels from Kondo satellite peaks near E_F, (iv) find that the Ce $4f$ c-electron hybridization in CeRhIn$_5$ is band dependent with the strongest hybridization on the most 3D band, and it is the weakest compared with those of CeCoIn$_5$ and CeIrIn$_5$, and (v) argue that the FS enlargement is minimal in the investigated T range.

High-quality single crystals of CeRhIn$_5$ were grown by the self-flux method [25]. The soft x-ray ARPES data in Figs. 1 and 2 were taken at the Advanced Resonant Spectroscopies (ADRESS) beam line at the Swiss Light Source; the overall energy resolution was 70–80 meV, and the angular resolution was 0.07°. The samples were cleaved and measured at 12 K under a vacuum better than 5×10^{-11} mbar. The resonant photoemission data were taken with 121 eV photons at beam line I05-ARPES at the Diamond Light Source. The angular resolution was 0.2°, and the overall energy resolution was better than 17 meV. The samples were cleaved at 8 K, and the vacuum was below 9×10^{-11} mbar.

The 3D electronic structure of CeRhIn$_5$ was measured with soft x-ray ARPES and compared with calculations when taking f electrons as fully localized in Fig. 1(a). Photoemission intensity maps in the ΓZAM and ΓZRX planes are shown in Figs. 1(b) and 1(c), respectively. Different k_z's were accessed by varying the photon energy between 532 and 648 eV, and estimated based on an inner potential of 15 eV [26]. As elaborated in the Supplemental Material [26], according to the "universal curve" of the electron mean free path as a function of kinetic energy [35], the probing depth here is larger than ~14 Å, and the k_z-broadening is less than ~8.5% $2\pi/c$, with c being the lattice constant of CeRhIn$_5$, which enables a proper measurement of the bulk 3D band structure [26,36]. The FS in the ΓXM plane, shown in Fig. 1(d), is composed of four pockets. There are three electron pockets around M: a flower-shaped β pocket, a rounded α pocket and a large square-like γ
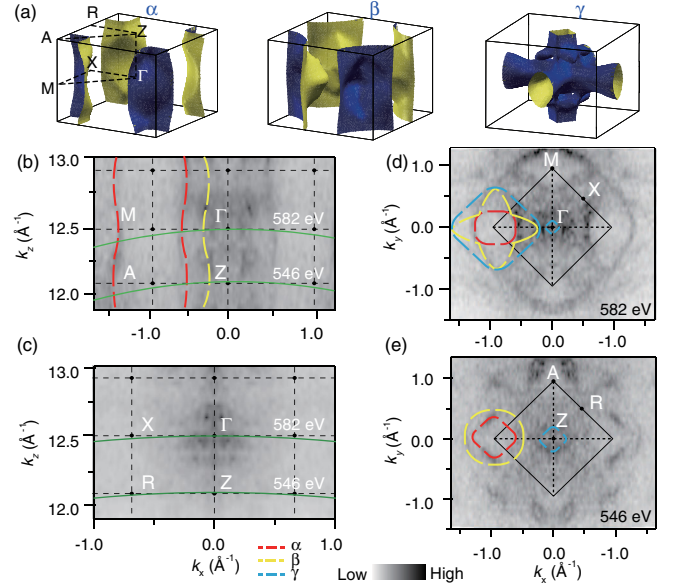

FIG. 1.   FSs of CeRhIn$_5$ at 12 K. (a) Calculated α, β, and γ FSs of CeRhIn$_5$, when considering fully localized f electrons [25]. (b),(c) Photoemission intensity maps in the (b) ΓZAM and (c) ΓZRX planes. The dispersion of γ is not marked due to its pronounced k_z dependence. The momentum cuts taken with 546 and 582 eV photons have been marked with the green solid lines in (b) and (c). (d),(e) Photoemission intensity maps in the (d) ΓXM and (e) ZAR planes taken with 582 and 546 eV photons. All data were integrated over a window of $(E_F - 20 \text{ meV}, E_F + 20 \text{ meV})$.

pocket. A small hole pocket can be observed around Γ, which is attributed to the γ band [Fig. 2(b)]. As shown by the band structure along ΓM in Fig. 2(a), α appears V-shaped with its bottom 1.3 eV below E_F. In the ZAR plane [Fig. 1(e)], the β pocket becomes rounded and the α pocket becomes square-like. For the photoemission data along ZA in Fig. 2(c), the bottom of α shifts toward E_F, while β gets closer to α. As shown in Figs. 2(b) and 1(d), γ encloses the Γ point forming the square-like Fermi pocket around the zone center.

Differences exist between the FSs in the ΓXM and ZAR planes for the three bands. The α and β FSs show weak variation in the ΓZAM plane [Fig. 1(b)], and α is the most two-dimensional (2D), while γ exhibits the strongest k_z dependence. The shapes of the α and β pockets are even qualitatively compatible with previous dHvA measurements in the magnetic phase [15]. These measurements, however, could not provide the shape and k_z dependence of γ, due to the low frequency of this branch, making the more comprehensive 3D electronic structure revealed by ARPES particularly useful. Most parts of the FSs and bands agree well with the DFT calculations for the paramagnetic phase, shown in Figs. 1(a) and 2(e), where the $4f$ electrons are treated as fully localized and Kondo spin scattering is neglected. This should reproduce the FSs when the effect of the coupling between $4f$ electrons and conduction
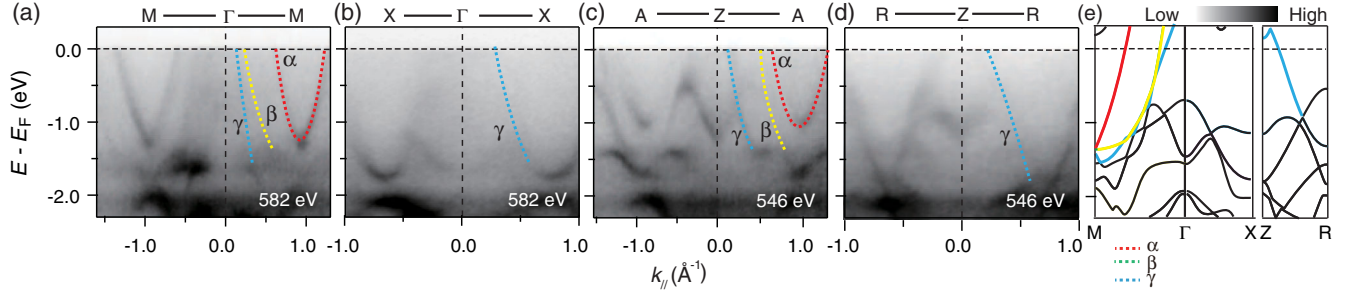
FIG. 2. Band structure of CeRhIn$_5$ at 12 K. (a)–(d) Photoemission intensity distributions along (a) ΓM, (b) ΓX, (c) ZA, and (d) ZR. The corresponding momentum cuts have been marked in Figs. 1(b) and 1(c). (e) Calculated band structure of CeRhIn$_5$ along high-symmetry directions, when considering fully localized f electrons and a paramagnetic phase. The bands are color coded as marked. The positions of the momentum cuts are marked in Figs. 1(b) and 1(c).

electrons is negligible. This agreement indicates that the $4f$ electrons indeed are predominantly localized. Still, differences between the DFT calculations and our measurements exist: the Fermi crossing of γ along ΓX in Fig. 2(b) is absent in Fig. 2(e). The calculation also indicates that all three conduction bands originate from the RhIn$_2$ layer, with α mainly composed of Rh $4d$ states, β mainly composed of In $5p$ states, and γ composed of both.

To enhance the f-electron photoemission intensity, resonant ARPES measurements were conducted at the Ce $4d - 4f$ transition with 121 eV photons. As shown in Fig. S2 of the Supplemental Material [26], the data taken with 882.5 eV photons at the $3d - 4f$ resonance are similar, but with a poor energy resolution. As further illustrated by Figs. S3 and S4 [26], the photons near $4d - 4f$ transition probe the bulk states as well, although the probing depth is about 7.5 Å, causing stronger k_z broadening. Figs. 3(a) and 3(b) compare the off-resonance and on-resonance photoemission intensities at 8 K, respectively. Strongly dispersing bands dominate the off-resonance spectra, while Ce $4f$ emission is enhanced in the on-resonance data; see also Fig. 3(d). Three nearly flat bands can be observed in the on-resonance data. The one at -2.32 eV is assigned to the $4f^0$ state, while those at -0.27 eV and near E_F have been attributed to the $4f_{7/2}^1$ and $4f_{5/2}^1$ states, respectively. The $4f$ spectral weight was found to be negligible near E_F in previous ARPES data on CeRhIn$_5$ [23]. Furthermore, we find that $4f_{5/2}^1$ is sensitive to the polarization—a significant enhancement is seen under s-polarized light compared with p polarization [Fig. 3(c)]. Figure 3(e) enlarges the energy distribution curves (EDCs) near E_F after dividing by the resolution-convoluted Fermi-Dirac distribution (RC-FDD), revealing two features at ~ 1.5 and 8 meV, which we interpret as Kondo satellite peaks arising from the CEF splittings. The polarization dependence arises from wave function symmetry. The $4f_{5/2}^1$ manifold splits into three doubly degenerate states in the tetragonal environment, namely $\Gamma_7^+ = \beta| \pm \frac{5}{2}\rangle - \alpha| \mp \frac{3}{2}\rangle$, $\Gamma_6 = | \pm \frac{1}{2}\rangle$, and $\Gamma_7^- = \alpha| \pm \frac{5}{2}\rangle + \beta| \mp \frac{3}{2}\rangle$. Here, $\alpha = 0.62$ and $\beta = 0.78$ were determined
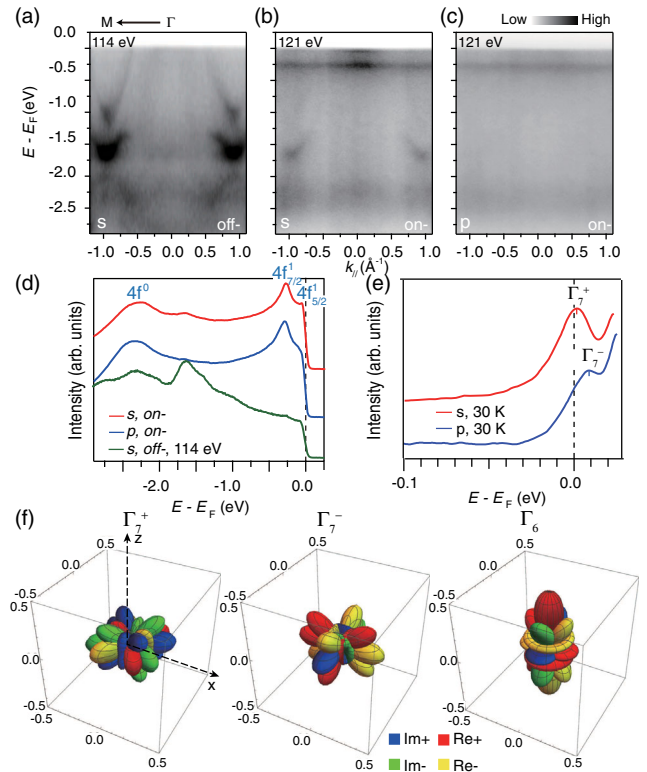

FIG. 3. Photoemission intensity distributions of CeRhIn$_5$ along ΓM taken at 8 K with (a) off-resonance (114 eV) s-polarized, (b) on-resonance (121 eV) s-polarized, and (c) on-resonance p-polarized photons. (d) Angle-integrated EDCs of CeRhIn$_5$ taken with off- and on-resonant energy; f-band positions are highlighted. (e) On-resonance EDCs of CeRhIn$_5$ taken at Γ with s- and p-polarized photons, after division by the RC-FDD. Labels follow the common notation in Refs. [23,38,39]. Momentum cuts with 121 eV photons cross $(0, 0, 7.07[(2\pi)/c])$, close to Γ, and are thus labeled $\Gamma - M$ for simplicity. (f) The distributions of the wave functions for the three doublets in the tetragonal crystal electric field, named Γ_7^+, Γ_7^-, and Γ_6, respectively. The positive and negative real and imaginary parts of the wave functions are color coded as marked.

by inelastic neutron scattering [37]. The corresponding distributions of these wave functions are displayed in Fig. 3(f). All these are somewhat elongated along z, allowing hybridization with the conduction electrons. Both Γ_7^+ and Γ_7^- have mixed even and odd components with respect to the xz plane (defining the x axis as the Ce-In-Ce direction and z as the c axis), while Γ_6 is even. Moreover, the odd component of Γ_7^+ is larger than its even component, while the reverse is true for Γ_7^-. Since s polarization picks up the odd components, the prominent state at 1.5 meV above E_F is assigned to Γ_7^+. The Kondo satellite state observed with p polarization at 8 meV above E_F is assigned to Γ_7^-. The observed separation of 6.5 meV between the two states agrees well with that from inelastic neutron scattering [37]. The third state, Γ_6, is too far above E_F (25 meV) to be resolved here. Thus, ARPES with polarized light can be a valuable complement to neutron scattering and specific heat measurements in determining the CEF states in Kondo systems. The $4f_{7/2}^1$ multiplet at higher binding energy features a broader line shape than the $4f_{5/2}^1$ one. Individual Kondo satellite peaks therefore were not resolved.

To investigate the degree of f-electron delocalization, we performed T-dependent measurements along ΓM; see Fig. 4(a). At high T, only two weak structures are observed—one at E_F, the other at around -0.27 eV. Upon cooling, the intensity of both features gradually increases until significant spectral weight can be observed near E_F at low T, particularly near Γ. This further corroborates the interpretation of both features as Kondo resonances which in principle should be detectable using STS [24,26].
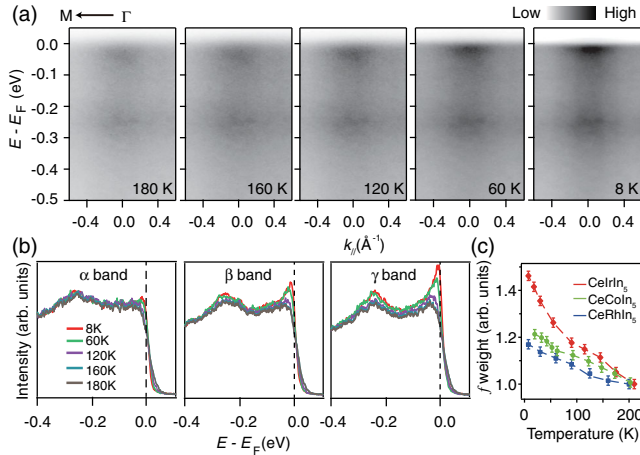
Figure 4(b) displays the EDCs at the Fermi crossings of α, β, and γ at low temperature. The $4f$ c-electron hybridization displays a clear band dependence—the most 2D α band shows negligible hybridization, while the most 3D γ band shows the strongest hybridization. This is consistent with both thermal expansion and DMFT results [37,41]. Consistently, a nearly flat band displaying a weak dispersion near Γ is clearly visible in the EDCs taken at 8 K near E_F due to the hybridization between the $4f$ band and γ; see Fig. 5(a). Figure 4(c) compares the T dependence of f spectral weight in the vicinity of Γ of CeRhIn$_5$ and those of its sister compounds CeCoIn$_5$ and CeIrIn$_5$. Obviously, the f spectral weight in CeRhIn$_5$ increases more slowly upon lowering T than those in CeCoIn$_5$ and CeIrIn$_5$, indicating that the hybridization is weakest in CeRhIn$_5$ among these compounds. In the Supplemental Material [26], we compare the band structure of the three compounds. An obvious band bending can be observed in α for CeCoIn$_5$ and CeIrIn$_5$, but not for CeRhIn$_5$ down to 8 K. In short, the $4f$ c hybridization weakens in the order of CeIrIn$_5$, CeCoIn$_5$, and CeRhIn$_5$.

Having firmly established that Kondo resonances do form in CeRhIn$_5$ as T is lowered, we now turn to a discussion of the size of the FS. It is important to note that the formation of Kondo resonances is not *per se* tantamount to the formation of a large FS. As sketched in Fig. 5(b), i.e., according to the standard view on the heavy fermion ground state, when f electrons hybridize with conduction electrons, the intensity of the f spectral weight will be redistributed, with significant enhancement to the "inside" of the hole-like and the "outside" of the electron-like bands. This is demonstrated by comparing the photoemission intensity maps of CeRhIn$_5$ taken at 8 and 180 K, respectively, in Figs. 5(c) and 5(d). The

FIG. 4. Temperature evolution of the electronic structure of CeRhIn$_5$. (a) Resonant ARPES data along ΓM at the temperatures indicated. (b) T dependence of the EDCs at the Fermi crossings of α, β, and γ. Thermal broadening near E_F is removed by dividing the spectra with the RC-FDD at corresponding temperatures and then multiplied by that of 8 K. (c) T dependence of the quasiparticle spectral weight near E_F in the vicinity of Γ for CeCoIn$_5$ [13], CeRhIn$_5$, and CeIrIn$_5$ [26,40], integrated over $[E_F - 40$ meV, $E_F + 20$ meV].
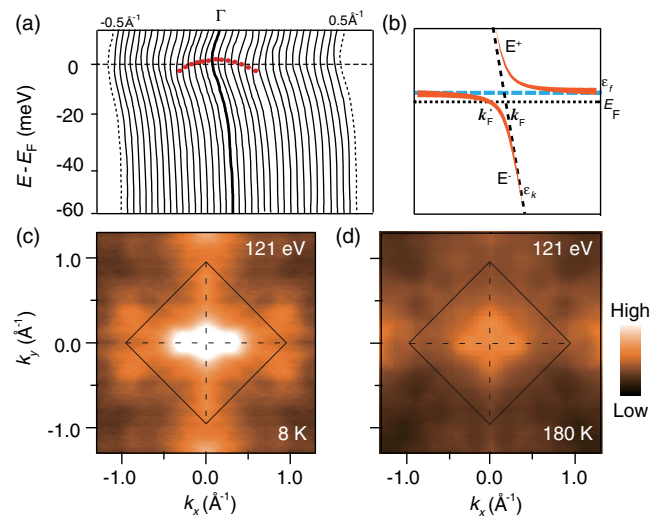
FIG. 5. Formation of the heavy quasiparticle band in CeRhIn$_5$. (a) The EDCs at 8 K along ΓM, divided by the RC-FDD. (b) Schematic diagram of the hybridization between f electrons (ε_f) and a conduction band (ε_k) under a periodic Anderson model. The orange curve is the hybridized band. (c), (d) Photoemission intensity maps at (c) 8 and (d) 180 K.

change of the Fermi wave vector from k_F, the Fermi wave vector of the so-called "small" FS with the f moments being localized, to k_F' of the "large" FS entails a reduction of spectral weight at k_F according to Fig. 5(b). Although there are signs for hybridization in Figs. 4 and 5(a), this reduction is not observed down to the lowest T of our experiment; see Fig. 5(c). Therefore, our findings indicate that the enlargement of the Fermi surface is minimal, and it is still predominantly "small" in CeRhIn$_5$ at ambient pressure down to 8 K despite the formation of a flat band near E_F [18,25], and they also clarify why some experiments on CeRhIn$_5$ have been interpreted in terms of complete $4f$-electron delocalization and do show how subtle the issue of large vs small FS can be.

In conclusion, we demonstrate that polarization-dependent ARPES could extract information about the CEF levels in CeRhIn$_5$. We showed that there is band-dependent $4f$ c hybridization, and the FS in the paramagnetic phase of CeRhIn$_5$ is predominantly small down to 8 K, although a narrow band forms near E_F as a result of Kondo scattering. These findings clarify why different experiments have seemingly obtained conflicting results regarding the fate of the Kondo effect in CeRhIn$_5$. Our findings give a comprehensive electronic structure of CeRhIn$_5$, and the comparison with CeCoIn$_5$ and CeIrIn$_5$ aids a global understanding of the CeMIn$_5$ family which epitomizes the richness of strongly correlated electron systems [42].

---

[*]stefan.kirchner@correlated-matter.com

[†]dlfeng@fudan.edu.cn

[1] G. R. Stewart, Rev. Mod. Phys. **56**, 755 (1984).

[2] Q. Si, J. H. Pixley, E. Nica, S. J. Yamamoto, P. Goswami, R. Yu, and S. Kirchner, J. Phys. Soc. Jpn. **83**, 061005 (2014).

[3] P. Coleman and A. H. Nevidomskyy, J. Low Temp. Phys. **161**, 182 (2010).

[4] S. Doniach, Physica (Amsterdam) **91B+C**, 231 (1977).

[5] V. A. Sidorov, M. Nicklas, P. G. Pagliuso, J. L. Sarrao, Y. Bang, A. V. Balatsky, and J. D. Thompson, Phys. Rev. Lett. **89**, 157004 (2002).

[6] T. Mito, S. Kawasaki, Y. Kawasaki, G.-Q. Zheng, Y. Kitaoka, D. Aoki, Y. Haga, and Y. Ōnuki, Phys. Rev. Lett. **90**, 077004 (2003).

[7] C. Petrovic, P. G. Pagliuso, M. F. Hundley, R. Movshovich, J. L. Sarrao, J. D. Thompson, Z. Fisk, and P. Monthoux, J. Phys. Condens. Matter **13**, L337 (2001).

[8] C. Petrovic, R. Movshovich, M. Jaime, P. G. Pagliuso, M. F. Hundley, J. L. Sarrao, Z. Fisk, and J. D. Thompson, Europhys. Lett. **53**, 354 (2001).

[9] H. Hegger, C. Petrovic, E. G. Moshopoulou, M. F. Hundley, J. L. Sarrao, Z. Fisk, and J. D. Thompson, Phys. Rev. Lett. **84**, 4986 (2000).

[10] S.-I. Fujimor, A. Fujimori, K. Shimada, T. Narimura, K. Kobayashi, H. Namatame, M. Taniguchi, H. Harima, H. Shishido, S. Ikeda, D. Aoki, Y. Tokiwa, Y. Haga, and Y. Ōnuki, Phys. Rev. B **73**, 224517 (2006).

[11] A. Koitzsch, T. K. Kim, U. Treske, M. Knupfer, B. Büchner, M. Richter, I. Opahle, R. Follath, E. D. Bauer, and J. L. Sarrao, Phys. Rev. B **88**, 035124 (2013).

[12] A. Koitzsch, S. V. Borisenko, D. Inosov, J. Geck, V. B. Zabolotnyy, H. Shiozawa, M. Knupfer, J. Fink, B. Büchner, E. D. Bauer, J. L. Sarrao, and R. Follath, Phys. Rev. B **77**, 155128 (2008).

[13] Q. Y. Chen, D. F. Xu, X. H. Niu, J. Jiang, R. Peng, H. C. Xu, C. H. P. Wen, Z. F. Ding, K. Huang, L. Shu, Y. J. Zhang, H. Lee, V. N. Strocov, M. Shi, F. Bisti, T. Schmitt, Y. B. Huang, P. Dudin, X. C. Lai, S. Kirchner, H. Q. Yuan, and D. L. Feng, Phys. Rev. B **96**, 045107 (2017).

[14] K. Haule, C. H. Yee, and K. Kim, Phys. Rev. B **81**, 195107 (2010).

[15] H. Shishido, R. Settai, D. Aoki, S. Ikeda, H. Nakawaki, N. Nakamura, T. Iizuka, Y. Inada, K. Sugiyama, T. Takeuchi, K. Kindo, T. C. Kobayashi, Y. Haga, H. Harima, Y. Aoki, T. Namiki, H. Sato, and Y. Ōnuki, J. Phys. Soc. Jpn. **71**, 162 (2002).

[16] N. Harrison, U. Alver, R. G. Goodrich, I. Vekhter, J. L. Sarrao, P. G. Pagliuso, N. O. Moreno, L. Balicas, Z. Fisk, D. Hall, R. T. Macaluso, and J. Y. Chan, Phys. Rev. Lett. **93**, 186405 (2004).

[17] F. P. Mena, D. van der Marel, and J. L. Sarrao, Phys. Rev. B **72**, 045119 (2005).

[18] H. Shishido, R. Settai, H. Harima, and Y. Ōnuki, J. Phys. Soc. Jpn. **74**, 1103 (2005).

[19] P. Coleman, C. Pepin, Q. Si, and R. Ramazashvili, J. Phys. Condens. Matter **13**, R273 (2001).

[20] Q. Si, S. Rabello, K. Ingersent, and J. L. Smith, Nature (London) **413**, 804 (2001).

[21] K. Miyake and H. Ikeda, J. Phys. Soc. Jpn. **75**, 033704 (2006).

[22] D. P. Moore, T. Durakiewicz, J. J. Joyce, A. J. Arko, L. A. Morales, J. L. Sarrao, and P. G. Pagliuso, J. M. Wills, and C. G. Olson, Physica (Amsterdam) **312B-313B**, 134 (2002).

[23] S. I. Fujimori, T. Okane, J. Okamoto, K. Mamiya, Y. Muramatsu, A. Fujimori, H. Harima, D. Aoki, S. Ikeda, H. Shishido, Y. Tokiwa, Y. Haga, and Y. Ōnuki, Phys. Rev. B **67**, 144507 (2003).

[24] P. Aynajian, E. H. da Silva Neto, A. Gyenis, R. E. Baumbach, J. D. Thompson, Z. Fisk, E. D. Bauer, and A. Yazdani, Nature (London) **486**, 201 (2012).

[25] L. Jiao, Y. Chen, Y. Kohama, D. Graf, E. D. Bauer, J. Singleton, J.-X. Zhu, Z. Weng, G. Pang, T. Shang, J. Zhang, H. Lee, T. Park, M. Jaime, J. D. Thompson, F. Steglich, Q. Si, and H. Q. Yuan, Proc. Natl. Acad. Sci. USA **112**, 673 (2015).

[26] See Supplemental Material at http://link.aps.org/supplemental/10.1103/PhysRevLett.120.066403 for Band-dependent interlayer f-electron hybridization in CeRhIn$_5$, which includes Refs. [27–34].

[27] Y. Chen, Front. Phys. **7**, 175 (2012).

[28] A. Damascelli, Z. Hussain, and Z.-X. Shen, Rev. Mod. Phys. **75**, 473 (2003).

[29] T. Ito, P. A. Rayjada, N. Kamakura, Y. Takata, T. Yokoya, A. Chainani, S. Shin, M. Hohara, and H. Takagi, J. Phys. Condens. Matter **15**, S2149 (2003).

[30] D. Ehm, F. Reinert, G. Nicolay, S. Schmidt, S. Hüfner, R. Claessen, V. Eyert, and C. Geibel, Phys. Rev. B **64**, 235104 (2001).

[31] J. D. Denlinger, G.-H. Gweon, J. W. Allen, C. G. Olson, M. B. Maple, J. L. Sarrao, P. E. Armstrong, Z. Fisk, and H. Yamagami, J. Electron Spectrosc. Relat. Phenom. **117–118**, 347 (2001).

[32] V. N. Strocov, J. Electron Spectrosc. Relat. Phenom. **130**, 65 (2003).

[33] H. Wadati, T. Yoshida, A. Chikamatsu, H. Kumigashira, M. Oshima, H. Eisaki, Z.-X. Shen, T. Mizokawa, and A. Fujimor, Phase Transitions **79**, 617 (2006).

[34] A. C. Hewson, *The Kondo Problem to Heavy Fermions* (Cambridge University Press, Cambridge, England, 1993).

[35] S. I. Fujimori, Y. Takeda, T. Okane, Y. Saitoh, A. Fujimori, H. Yamagami, Y. Haga, E. Yamamoto, and Y. Ōnuki, J. Phys. Soc. Jpn. **85**, 062001 (2016).

[36] A. Damascelli, Phys. Scr. **T109**, 61 (2004).

[37] T. Willers, Z. Hu, N. Hollmann, P. O. Körner, J. Gegner, T. Burnus, H. Fujiwara, A. Tanaka, D. Schmitz, H. H. Hsieh, H. J. Lin, C. T. Chen, E. D. Bauer, J. L. Sarrao, E. Goremychikin, M. Koza, L. H. Tjeng, and A. Severing, Phys. Rev. B **81**, 195114 (2010).

[38] H. J. Im, T. Ito, H.-D. Kim, S. Kimura, K. E. Lee, J. B. Hong, Y. S. Kwon, A. Yasui, and H. Yamagami, Phys. Rev. Lett. **100**, 176402 (2008).

[39] S. Patil, A. Generalov, M. Güttler, P. Kushwaha, A. Chikina, K. Kummer, T. C. Rödel, A. F. Santander-Syro, N. Caroca-Canales, C. Geibel, S. Danzenbächer, Y. Kucherenko, C. Laubschat, J. W. Allen, and D. V. Vyalikh, Nat. Commun. **7**, 11029 (2016).

[40] Q. Y. Chen *et al.*, Tracing crystal-field splittings in the rare earth-based intermetallic CeRhIn$_5$ (unpublished).

[41] N. Oeschler, P. Gegenwart, M. Lang, R. Movshovich, J. L. Sarrao, J. D. Thompson, and F. Steglich, Phys. Rev. Lett. **91**, 076402 (2003).

[42] It will be interesting to address how our findings relate to the intriguing finite field behavior of CeRhIn$_5$ [43].

[43] F. Ronning, T. Helm, K. Shirer, M. Bachmann, L. Balicas, B. J. Ramshaw, R. D. McDonald, F. F. Balakirev, M. Jaime, E. D. Bauer, and P. J. W. Moll, Nature (London) **548**, 313 (2017).

Correction: The omission of a support statement in the Acknowledgments section has been fixed.